Supplemental material for:

Protein structure prediction using sparse NOE and RDC restraints with Rosetta in CASP13

Georg Kuenze[1,2] & Jens Meiler*[1,2]

[1]Department of Chemistry, Vanderbilt University, Stevenson Center, Station B 351822, Nashville, TN 37232, USA
[2]Center for Structural Biology, Vanderbilt University, 465 21st Ave, 5140 MRB3, Nashville, TN 37240, USA

Table of Contents

Supporting Methods

Method S1: Detailed description of the input format and application of the used NMR restraints

NOE and EC distance restraints (usually referred to as 'constraints' in Rosetta) and dihedral angle restraints are implemented through Rosetta's constraint framework and can be used with many popular modeling applications, e.g. *de novo* structure prediction, model scoring, comparative modeling or docking, via command line options. RDC restraints are implemented through an additional NMR framework and have a similar set of input options.

In the following section, we provide a detailed description of the input format and scoring procedure for the used NMR restraints, and indicate the interfaces through which they are applied in Rosetta modeling. Additional information on Rosetta's application for *de novo* structure prediction and comparative modeling including the use of experimental restraints can be found under the following links:

De novo structure prediction:

https://www.rosettacommons.org/demos/latest/tutorials/advanced_denovo_structure_prediction/folding_tutorial

https://www.rosettacommons.org/docs/latest/application_documentation/structure_prediction/abinitio

https://www.rosettacommons.org/docs/latest/application_documentation/structure_prediction/abinitio-relax

Comparative modeling:

https://www.rosettacommons.org/docs/latest/application_documentation/structure_prediction/RosettaCM

https://www.rosettacommons.org/docs/latest/scripting_documentation/RosettaScripts/Movers/movers_pages/HybridizeMover

A) NOE restraints

Non-ambiguous NOE contacts were used as 'strong' distance restraints with a flat-bottom bounded penalty function (eq.1):

$$f(x) = \begin{cases} \left(\frac{x-lb}{sd}\right)^2 & for\ x < lb \\ 0 & for\ lb \le x \le ub \\ \left(\frac{x-ub}{sd}\right)^2 & for\ ub < x \le ub + rswitch \cdot sd \\ \frac{1}{sd}\left(x - (ub + rswitch \cdot sd)\right) + \left(\frac{rswich \cdot sd}{sd}\right)^2 & for\ x > ub + rswitch \cdot sd \end{cases} \quad \text{(eq. 1)}$$

The score is zero when the atom pair distance x is within the lower (lb) and upper (ub) bound, but grows quadratically outside of that range (with a sloped defined by the standard deviation sd). At distances larger than $x > ub + rswitch \cdot sd$ the score increases linearly.

Ambiguous NOE contacts were incorporated with a sigmoidal penalty function (eq. 2) in low-resolution 'centroid' modeling stages or as group of nested restraints with a bounded penalty (eq. 1) in high-resolution full-atom modeling stages.

$$f(x) = \frac{1}{1+\exp(-m\cdot(x-x_0))} - 0.5 \quad \text{(eq. 2)}$$

Equation 2 was additionally offset by a value of -0.5 such that the restraint score fell within the range from -1 (satisfied) to 0 (not satisfied). In the present work, the sigmoidal function was centered at a Cβ-Cβ distance (Cα for glycine) of $x_0 = 8$ Å and had a slope of $m = 1$.

Displayed below are example sections from centroid and full-atom distance restraint files as implemented in Rosetta. In the centroid phase, a NOE contact was defined by an **`AtomPair`** distance restraint line in the Rosetta input file with a bounded (non-ambiguous NOE) or sigmoidal (ambiguous NOE) penalty function. NOE contacts involving a sidechain H-atom were mapped onto the respective residue's centroid (CEN) atom, and the upper bound of the restraint was increased to $ub + h$ where h is the number of methyl groups involved in the restraint (0, 1 or 2). In full-atom modeling, NOEs between single protons (e.g. H^N protons) were defined by **`AtomPair`** distance restraints in the Rosetta input file whereas for NOEs involving groups of equivalent or non-stereochemically assigned protons (e.g. methyl groups) an **`AmbiguousNMRDistance`** restraint was used. In this case, groups of protons are referred to by their pseudoatom names and the model-predicted NOE distance is calculated by applying r^{-6} distance averaging. Furthermore, in full-atom modeling, ambiguous NOE contacts (i.e. those NOEs which included more than one residue pair) were represented as a group of nested restraints. In this case, the **`AtomPair`** (or **`AmbiguousNMRDistance`**) restraints of the ambiguous NOE are listed on multiple lines, with the keyword **`AmbiguousConstraint`** opening the block and the keyword **`END`** ending the block.

Example file 1: NOE centroid atom pair distance restraint file (e.g. `T0957s1.noe.cen.cst`)

```
# BOUNDED distance restraint for unambiguous NOE contacts
# AtomPair Atom1_Name Atom1_Residue Atom2_Name Atom2_Residue BOUNDED Lower_Bound Upper_Bound SD NOE
#
AtomPair  CEN 115    H   4 BOUNDED 1.5 7.0 0.5 NOE
AtomPair  CEN 148    H 154 BOUNDED 1.5 7.0 0.5 NOE
AtomPair    H  22  CEN 115 BOUNDED 1.5 7.0 0.5 NOE
...
#
# SIGMOID penalty function for ambiguous NOE contacts, additionally weighted by ambiguity level
# AtomPair Atom1_Name Atom1_Residue Atom2_Name Atom2_Residue SCALARWEIGHTEDFUNC Weight
# SUMFUNC Number_Funcs 2 CONSTANTFUNC Constant_Value SIGMOID Center Slope
#
AtomPair   CB 118   CB  25 SCALARWEIGHTEDFUNC 0.500000 SUMFUNC 2 CONSTANTFUNC -0.5 SIGMOID 8.0 1.0
AtomPair   CB 110   CB  85 SCALARWEIGHTEDFUNC 0.333333 SUMFUNC 2 CONSTANTFUNC -0.5 SIGMOID 8.0 1.0
AtomPair   CB 128   CB 143 SCALARWEIGHTEDFUNC 0.333333 SUMFUNC 2 CONSTANTFUNC -0.5 SIGMOID 8.0 1.0
...
```

Example file 2: NOE full-atom pair distance restraint file (e.g. `T0957s1.noe.fa.cst`)

```
# BOUNDED distance restraint for unambiguous NOE contacts
# AtomPair Atom1_Name Atom1_Residue Atom2_Name Atom2_Residue BOUNDED Lower_Bound Upper_Bound SD NOE
#
AmbiguousNMRDistance  HD1 115    H   4 BOUNDED 1.5 6.0 0.5 NOE
AmbiguousNMRDistance  QQD 148    H 154 BOUNDED 1.5 6.0 0.5 NOE
AmbiguousNMRDistance    H  22  HD1 115 BOUNDED 1.5 6.0 0.5 NOE
...
# Group ambiguous NOE contacts in nested AmbiguousConstraint, score only the lowest energy contact
# AtomPair Atom1_Name Atom1_Residue Atom2_Name Atom2_Residue BOUNDED Lower_Bound Upper_Bound SD NOE
#
AmbiguousConstraint
AtomPair               H  27    H   5 BOUNDED 1.5 6.0 0.5 NOE
AtomPair               H  27    H  20 BOUNDED 1.5 6.0 0.5 NOE
AtomPair               H  27    H  21 BOUNDED 1.5 6.0 0.5 NOE
END
...
```

Atom pair distance restraints can be used e.g. with Rosetta's *de novo* prediction method (*minirosetta* application), for scoring of Rosetta models (*score_jd2* application) as well as for comparative modeling (with the *Hybridize* Mover that is accessible through the *rosetta_scripts* application) by adding the following command line options to the input file:

```
-constraints:cst_fa_file T0957s1.noe.fa.cst   # Atom pair distance restraint file
-constraints:cst_fa_weight 0.15               # Set weight for atom pair restraints

#-score:set_weights atom_pair_constraint 0.15 # Alternatively, set weight for atom pair restraints
                                              # with this option
```

B) EC restraints

Evolutionary couplings were incorporated as distance restraints between Cβ atoms (Cα for glycine) with a sigmoidal penalty function (eq. 2) centered at 8 Å and weighted by the EC confidence score.

Example file 3: EC distance restraints file (e.g. `T0957s1.ecs.csts`)

```
# SIGMOID penalty function for EC distance restraints
# AtomPair Atom1_Name Atom1_Residue Atom2_Name Atom2_Residue SCALARWEIGHTEDFUNC Weight
# SUMFUNC Number_Funcs 2 CONSTANTFUNC Constant_Value SIGMOID Center Slope
#
AtomPair   CB 132   CB 139 SCALARWEIGHTEDFUNC 0.879979 SUMFUNC 2 CONSTANTFUNC -0.5 SIGMOID 8.0 1.0
AtomPair   CB 127   CB 145 SCALARWEIGHTEDFUNC 0.856144 SUMFUNC 2 CONSTANTFUNC -0.5 SIGMOID 8.0 1.0
AtomPair   CB 139   CA 160 SCALARWEIGHTEDFUNC 0.836933 SUMFUNC 2 CONSTANTFUNC -0.5 SIGMOID 8.0 1.0
...
```

C) RDC restraints

RDCs were evaluated by calculating the molecular alignment tensor by singular value decomposition. The user has to prepare two files: 1) an input file with parameters to control the RDC score calculation (see example file 4), and 2) a column-formatted text file containing the measured RDC values for each alignment medium (see example file 5).

Example file 4: RDC input file (e.g. `T0957s1.rdc.inp`)

```
MULTISET
alignment_medium = Medium1
computation_type = SVD
alignment_tensor = [ -31.65, 0.11, 10.0, 10.0, 10.0 ] # Tensor values (Da,R,alpha,beta,gamma)
                                                       # If known tensor can be fixed, otherwise
                                                       # will be determined by SVD
dataset          = [ T0957s1_RDCs.1.cst, 1.0, SIGMA ] # RDC dataset file, weight, scale RDCs
                                                       # relative to their error
END
```

Example file 5: RDC data file (e.g. `T0957s1_RDCs.1.cst`)

```
# ( Residue Atom Chain Spin 1 ) ( Residue Atom Chain Spin 2 ) RDC Value RDC Error
#
(   5 H A ) (   5 N A )   6.19  3.0
(   6 H A ) (   6 N A ) -41.28  3.0
(   7 H A ) (   7 N A )  -8.91  3.0
(  11 H A ) (  11 N A )  32.94  3.0
(  14 H A ) (  14 N A )  33.54  3.0
```

```
(  16 H A ) (  16 N A )  35.75  3.0
(  17 H A ) (  17 N A )   6.71  3.0
(  18 H A ) (  18 N A )   3.10  3.0
(  19 H A ) (  19 N A ) -38.24  3.0
(  20 H A ) (  20 N A ) -43.22  3.0
...
```

Similar to distance restraints, RDC data can be used by adding the following options to the input file:

```
-score:weights ref2015              # Rosetta Ref2015 score function
-score:set_weights nmr_rdc 0.011    # Set weight for RDC score term

-nmr:rdc:input_file N0957s1.rdc.inp # RDC input file
-nmr:rdc:multiset_weights 1.0 1.0   # Weight different RDC datasets by these factors
-nmr:rdc:normalization_type none    # No need to normalize RDCs to N-H dipolar couplings
-nmr:rdc:correct_sign false         # Do not correct the sign of the 15N gyromagnetic ratio
```

Additional information on Rosetta's RDC scoring method and a list and explanation of all input options can be found under this link: https://www.rosettacommons.org/docs/latest/application_documentation/RosettaNMR-with-Paramagnetic-Restraints

D) Dihedral angle restraints

Dihedral angle restraints are formatted similar to distance restraints in Rosetta and are accessible through the same framework. In the restraint definition in the input file, dihedral angle ranges are usually expressed in radians and centered to the range -π to +π by applying a constant offset. Model-predicted dihedral angles are evaluated after offset correction. In this study, dihedral angle restraints were scored with a periodic bounded penalty function similar to equation 1. Below is an example of the Rosetta restraint file format.

Example file 6: Dihedral restraint file (e.g. `T0957s1_dihed.cst`)

```
# Dihedral Atom1_Name Atom1_Residue Atom2_Name Atom2_Residue Atom3_Name Atom3_Residue
# Atom4_Name Atom4_Residue OFFSETPERIODICBOUNDED Offset Period Lower_Bound Upper_Bound SD
# (values in radians)
#
# PHI
Dihedral C   4 N   5 CA   5 C   5 OFFSETPERIODICBOUNDED -1.929  6.283 -0.602  0.602  0.314
Dihedral C   5 N   6 CA   6 C   6 OFFSETPERIODICBOUNDED -1.929  6.283 -0.428  0.428  0.314
...
# PSI
Dihedral N   5 CA   5 C   5 N   6 OFFSETPERIODICBOUNDED  2.347  6.283 -0.602  0.602  0.314
Dihedral N   6 CA   6 C   6 N   7 OFFSETPERIODICBOUNDED  2.086  6.283 -0.515  0.515  0.314
...
```

Dihedral angle restraints were used in fragment picking by adding the following input options to the application and modifying the fragment picker weights file as shown below.

```
-constraints:cst_file T0957s1_dihed.cst
-frags:scoring:config fragment_picker_quota.wghts
```

Example file 7: Fragment picker weights file (e.g. `fragment_picker_quota.wghts`)

```
#score name priority weight min_allowed extras
SecondarySimilarity 350 0.5 - psipred
```

```
SecondarySimilarity 250 0.5 - jufo
RamaScore 150 1.0 - psipred
RamaScore 150 1.0 - jufo
ProfileScoreL1 200 1.0 -
DihedralConstraintsScore 100 5.0 -
```

More information on the Rosetta restraint framework and the restraint file format can be found under this link: https://www.rosettacommons.org/docs/latest/rosetta_basics/file_types/constraint-file

Supporting Figures

Figure S1: Richness and quality of the used NMR datasets

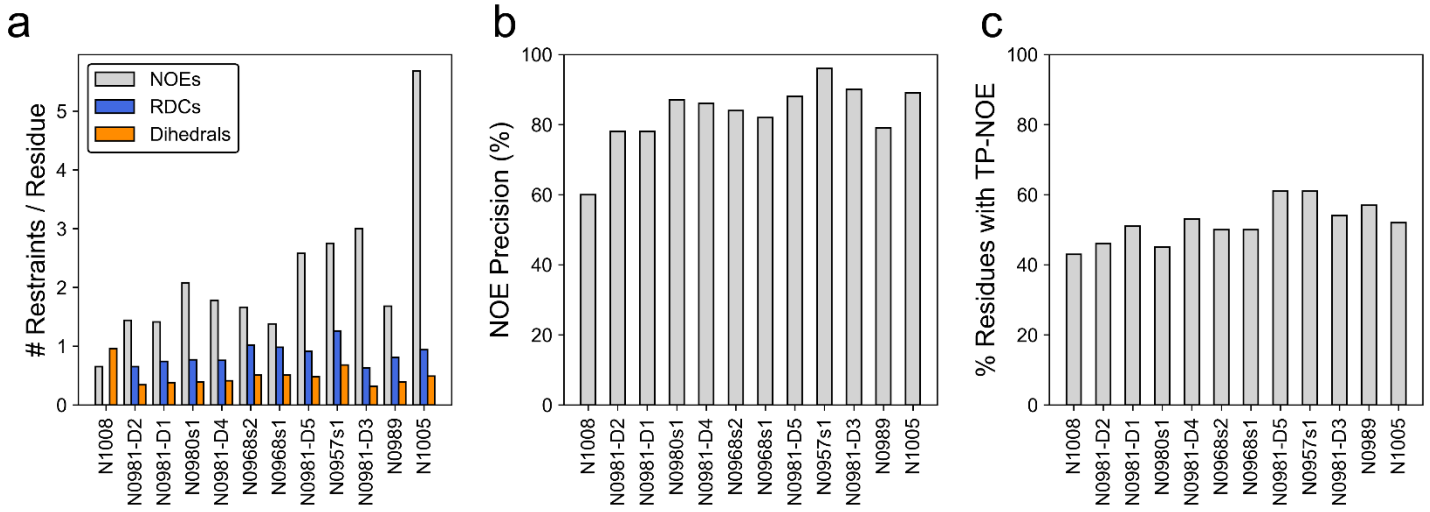

Figure S1: Richness and quality of the used NMR datasets. (a) Number of per-residue NOE, RDC and ϕ/ψ dihedral angle restraints which were employed in our NMR-assisted structure predictions. The average number of NOE, RDC and dihedral restraints was 2.2, 0.8 and 0.5 per residue, respectively. **(b)** NOE precision; defined as ratio of the number of true positive (TP)-NOEs to the total number of NOEs. The average NOE precision was 83%. **(c)** Fraction of protein residues which had at least one TP-NOE. The average over all prediction targets was 52%.

Figure S2: Local model accuracy of *de novo* predicted NMR-assisted targets

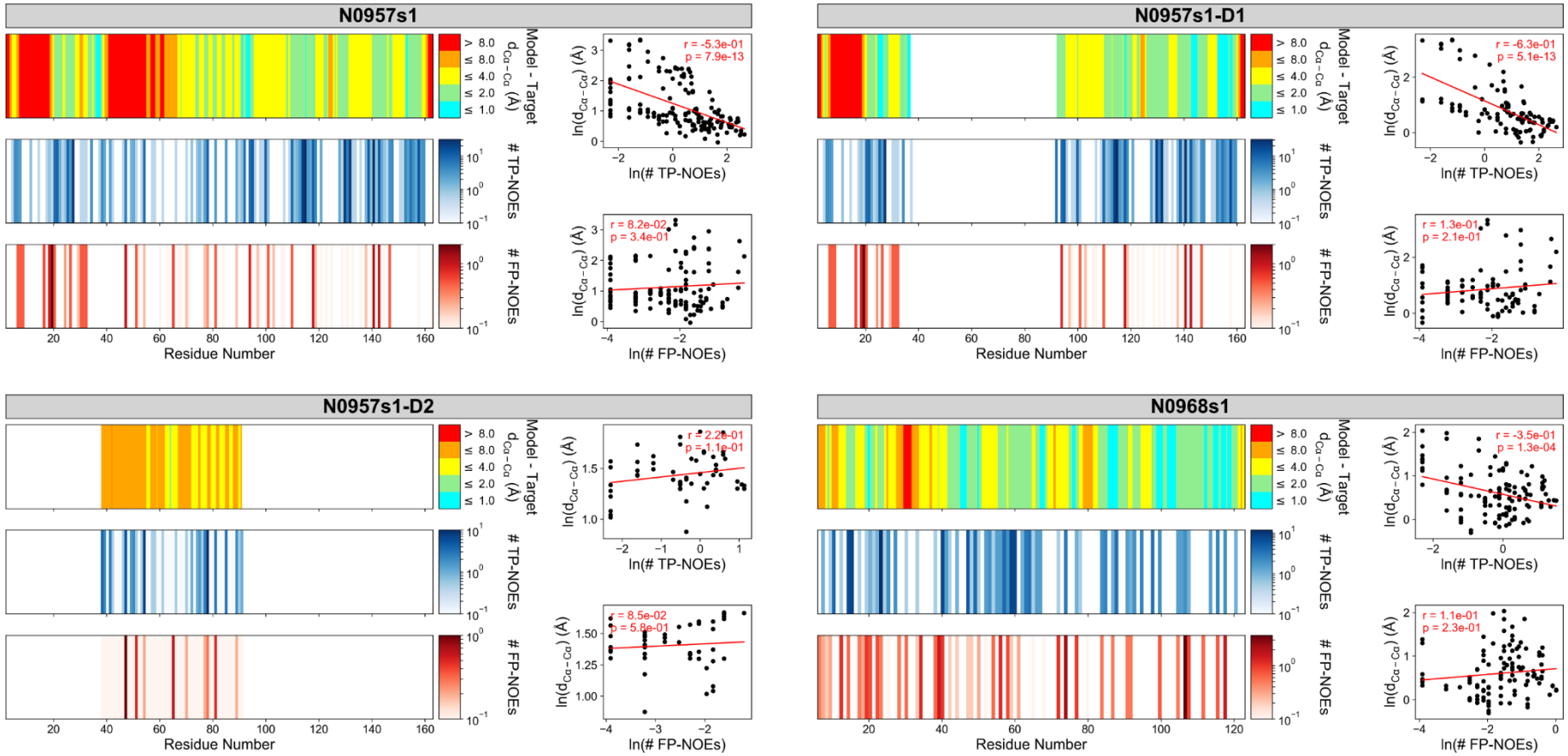

Figure S2: Comparison of local model accuracy of *de novo* predicted NMR-assisted targets to number and distribution of NOE restraints. For each of the 12 prediction targets or 16 evaluation units, respectively, the local Cα-Cα deviation between model and reference structure is compared to the number and location of true positive (TP) and false positive (FP) NOEs. For targets N0957s1 and N0989, data are also shown for separate domains. For each target, the panels display the following results: On the left side, the Cα-Cα distance between the submitted model 1 and the reference structure after superimposition with the program MAMMOTH[1] (top) and the number of TP (middle) and FP (bottom) NOEs versus the protein residue number are shown. On the right side, the natural logarithm of the Cα-Cα distance deviation (calculated as running average over five neighboring residues) is plotted versus the logarithm of the number of TP (top) and FP (bottom) NOEs. Red lines represent the least-squares fit to a linear regression model.

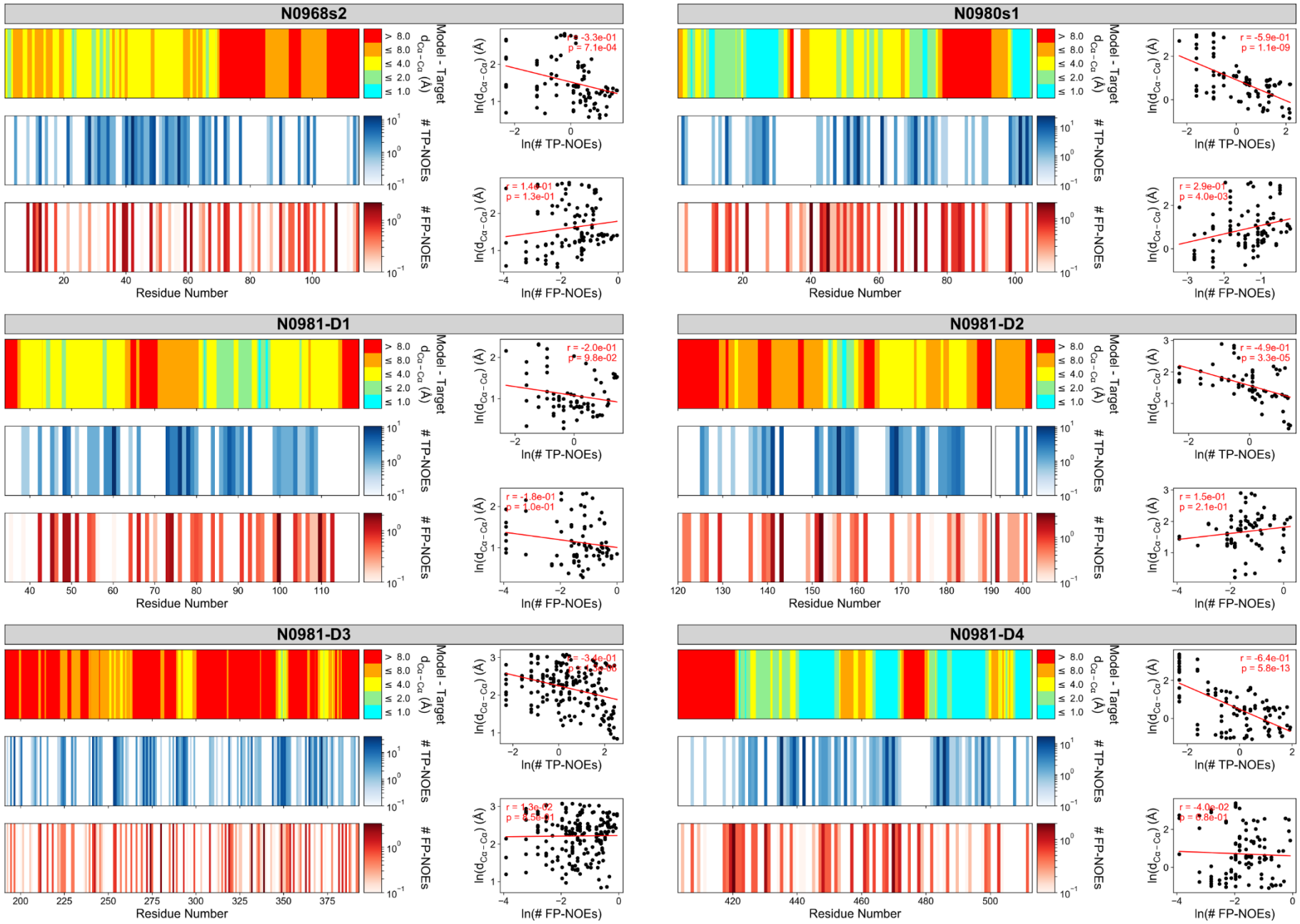

Figure S2: Comparison of local model accuracy of *de novo* predicted NMR-assisted targets to number and distribution of NOE restraints. (continued)

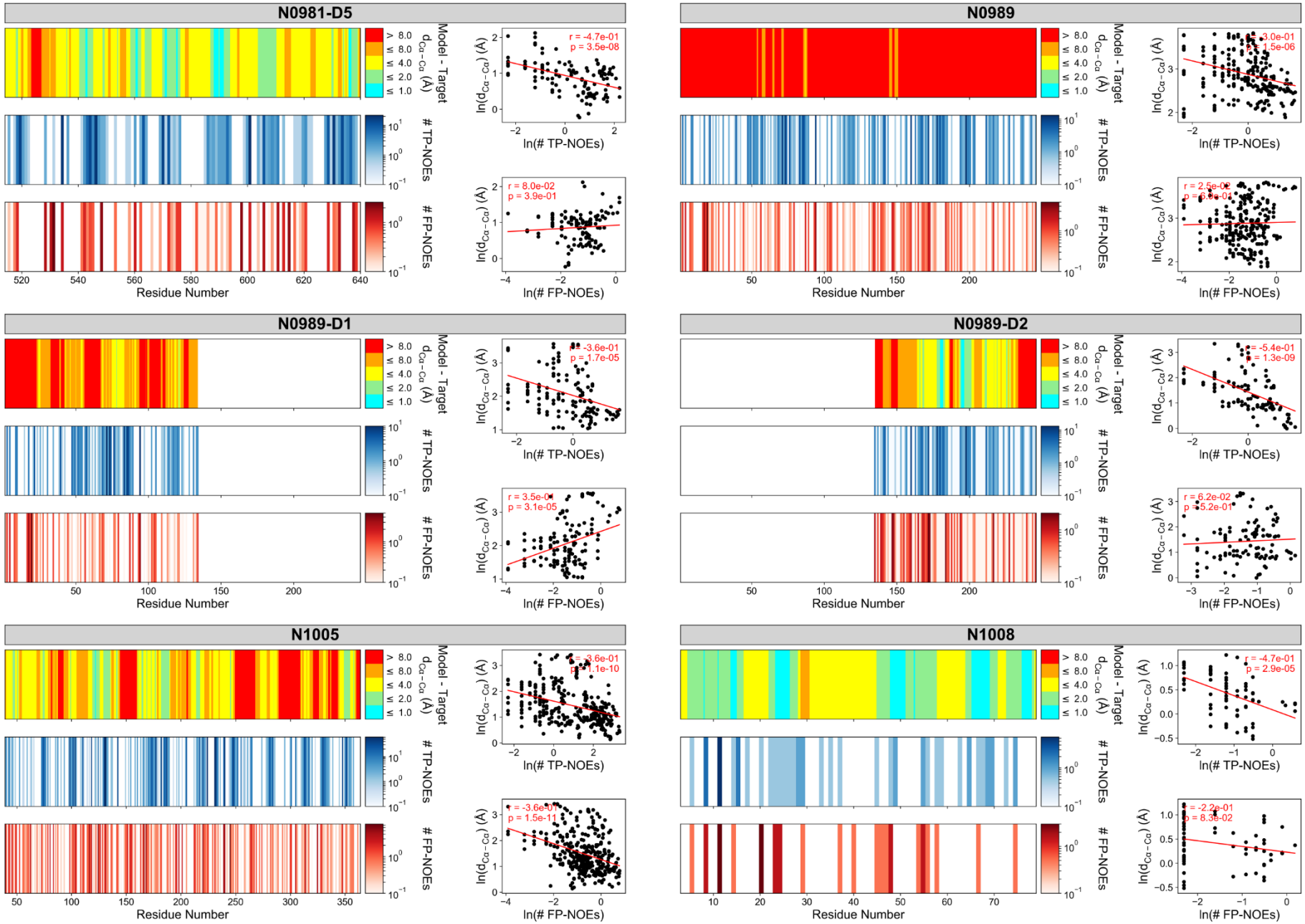

Figure S2: Comparison of local model accuracy of *de novo* predicted NMR-assisted targets to number and distribution of NOE restraints. (continued)

Figure S3: Local model accuracy of NMR-refined server-models from our post-CASP13 analysis

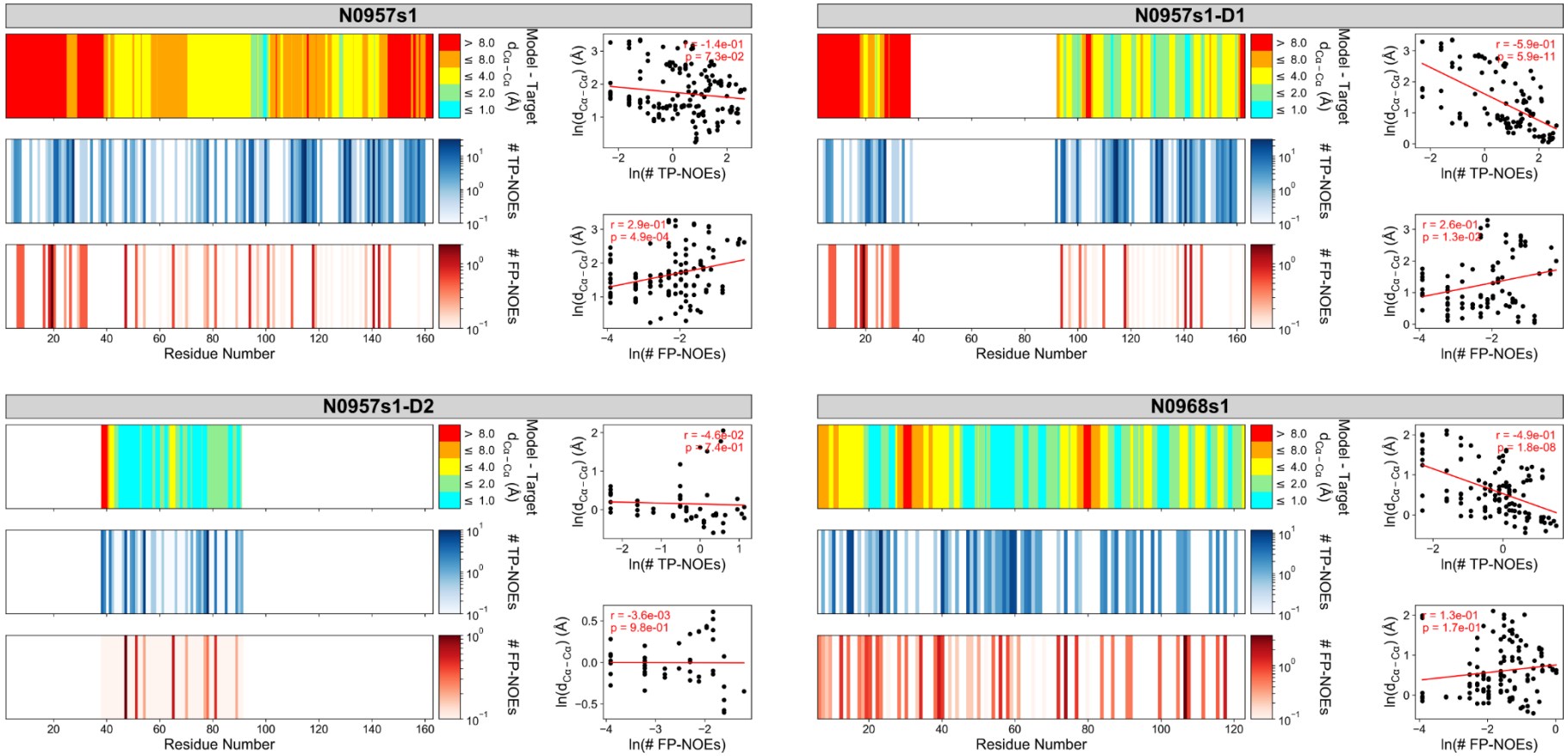

Figure S3: Comparison of local model accuracy of NMR-refined server-models from our post-CASP13 analysis to distribution and number of NOE restraints. Models were created by combining and refining the five submitted models from the I-TASSER[2,3], QUARK[4], Robetta[5], RaptorX-Contact[6] and RaptorX-TBM[7] server, respectively, with RosettaCM and NMR data. For each of the 12 prediction targets or 16 evaluation units, respectively, the local Cα-Cα deviation between the best scoring NMR-refined server-model and the reference structure is compared to the number and location of true positive (TP) and false positive (FP) NOEs. For targets N0957s1 and N0989, data are also shown for separate domains. The arrangement of panels is the same as in **Figure S2**: On the left side, the Cα-Cα distance between model and reference structure after superimposition with the program MAMMOTH[1] (top) and the number of TP (middle) and FP (bottom) NOEs versus the protein residue number are shown. On the right side, the natural logarithm of the Cα-Cα distance deviation (calculated as running average over five neighboring residues) is plotted versus the logarithm of the number of TP (top) and FP (bottom) NOEs. Red lines represent the least-squares fit to a linear regression model.

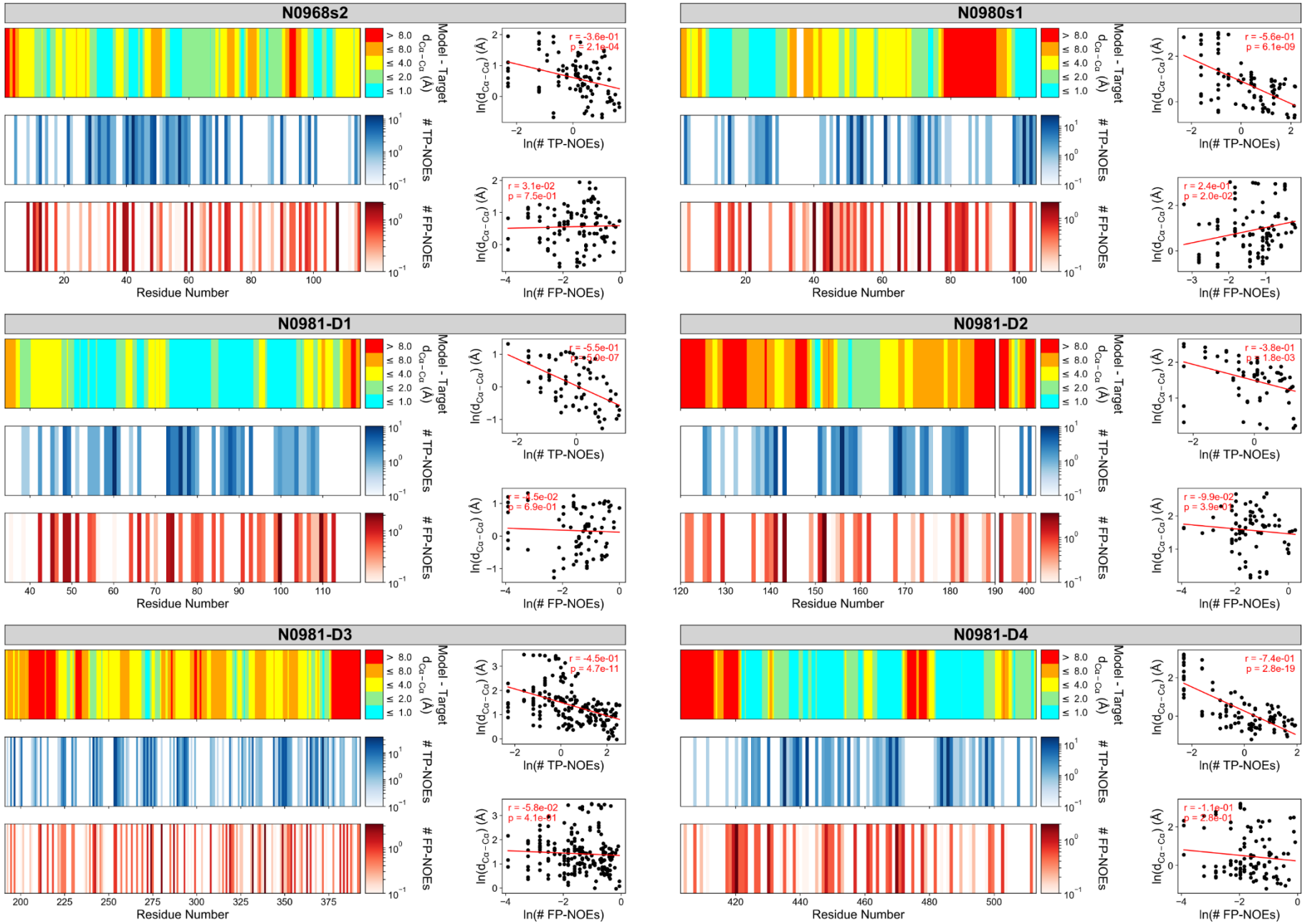

Figure S3: Comparison of local model accuracy of NMR-refined server-models from our post-CASP13 analysis to distribution and number of NOE restraints (continued).

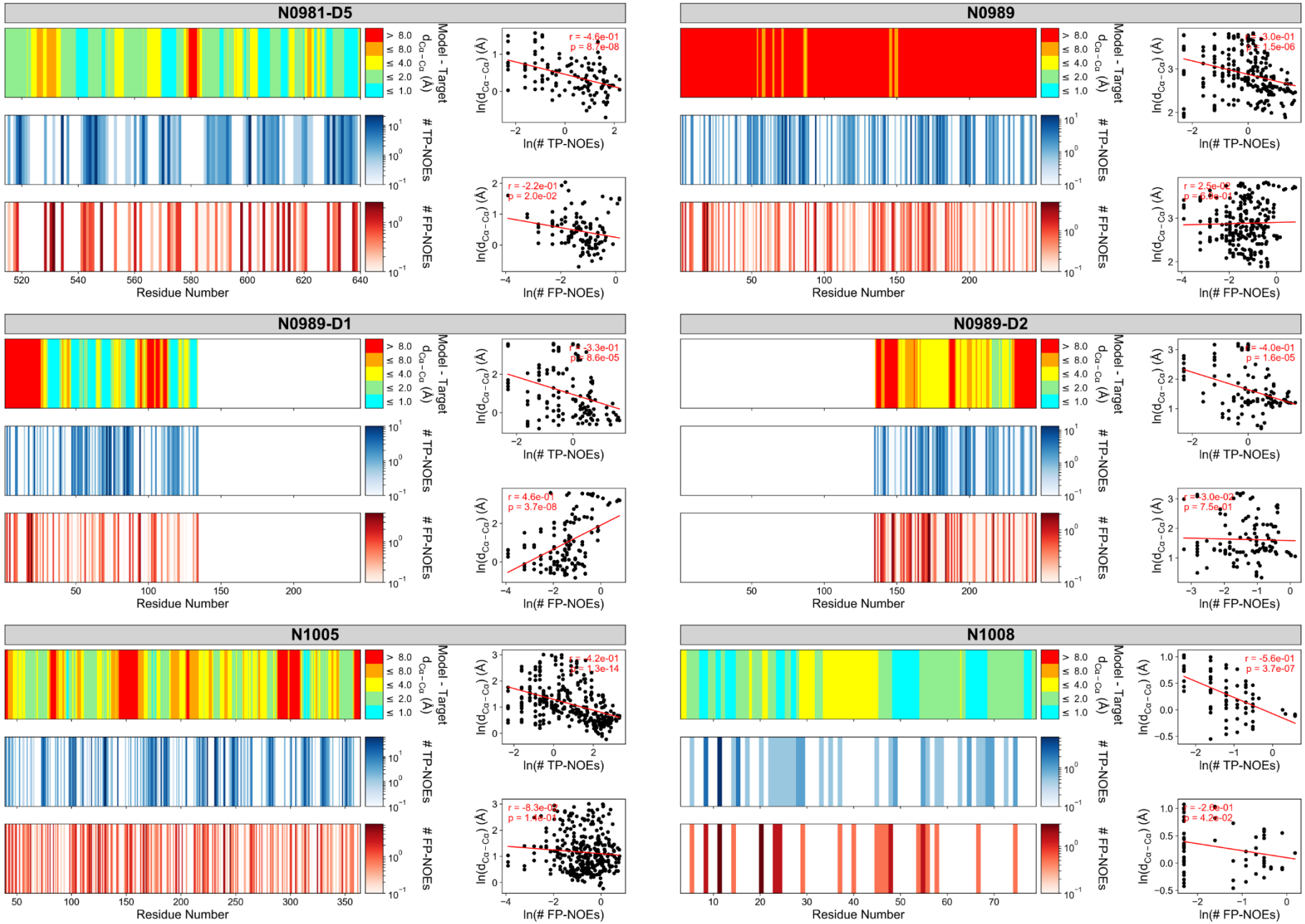

Figure S3: Comparison of local model accuracy of NMR-refined server-models from our post-CASP13 analysis to distribution and number of NOE restraints (continued).

Figure S4: Results of *de novo* structure prediction of NMR-assisted targets

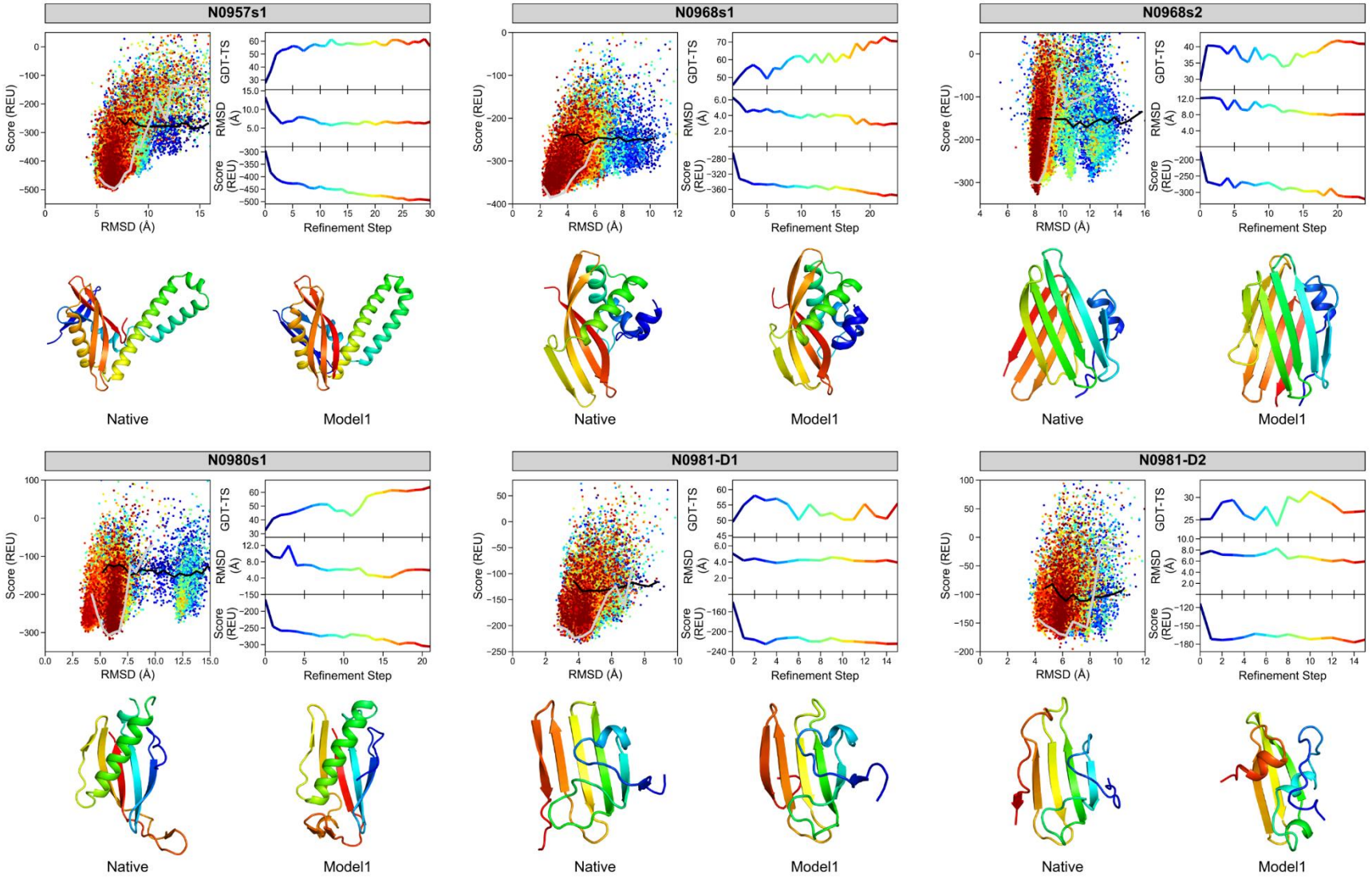

Figure S4: Results of *de novo* structure prediction of NMR-assisted (NOE+RDC) modeling targets in CASP13.

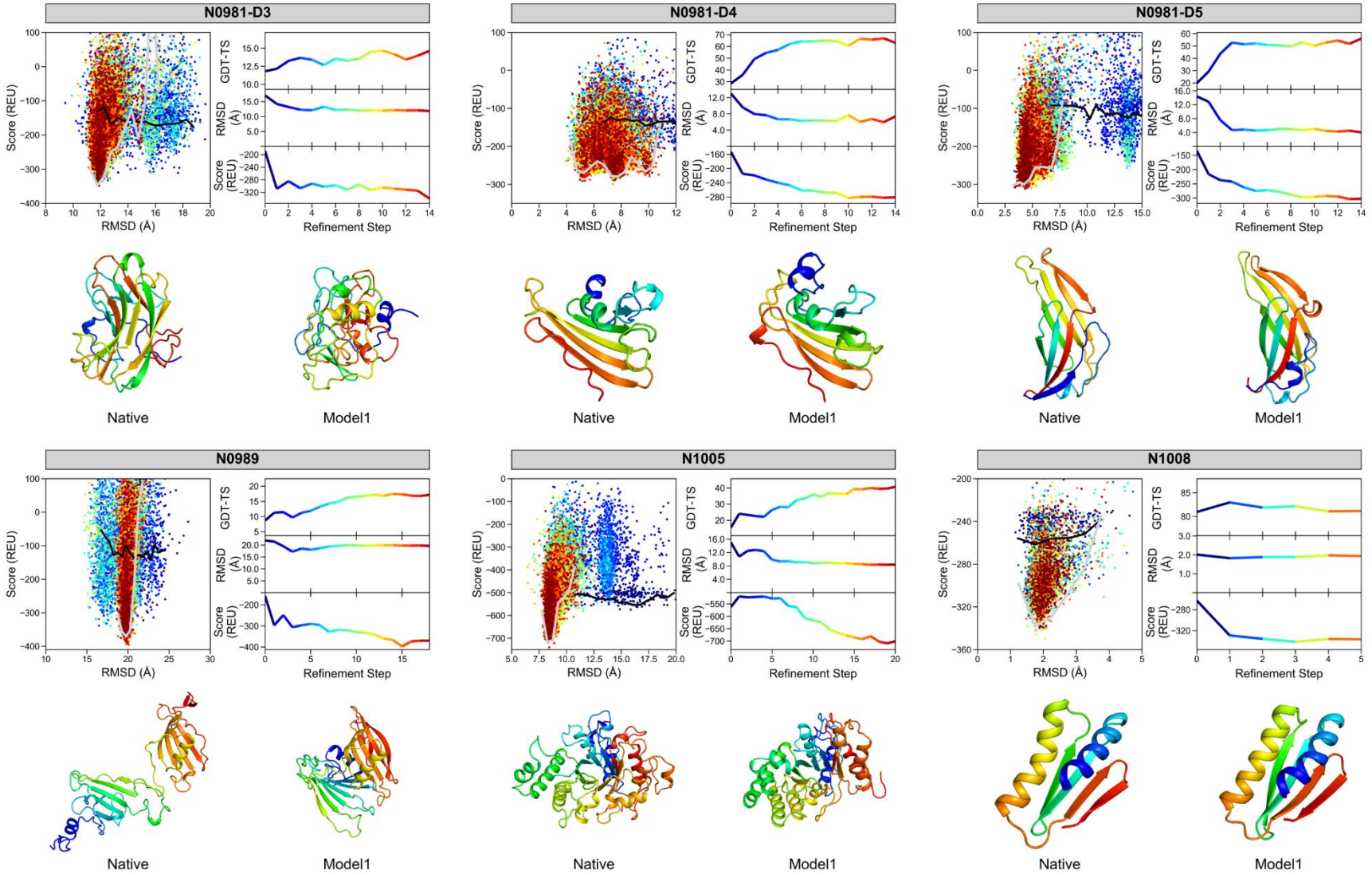

Figure S4: Results of *de novo* structure prediction of NMR-assisted (NOE+RDC) modeling targets in CASP13 (continued). Each of the 12 prediction targets was first folded with RosettaAbInitio and then iteratively refined with RosettaCM. The panels display the following results: The upper left panel plots the combined Rosetta energy and NMR NOE+RDC restraint score versus the model's Cα-RMSD relative to the reference structure. The color coding (blue to red) corresponds to the number of refinement steps. The black and gray line represent the lowest-energy rim (i.e. the median of the five lowest-scoring models by RMSD bin) of the score-vs-RMSD plot of the model pool before the first and after the final refinement step. Note that the pool at step 0 is comprised of models after the initial iterative hybridize selection step. The upper right panel displays the average GDT-TS (top row), Cα-RMSD (middle row) and score (bottom row) of the ten lowest scoring models after each refinement step. The values of successive refinement steps are colored from blue to red. The lower panel compares the experimental reference structure (left) depicted as ribbon diagram and colored in rainbow with the submitted model 1 (right) which was the best-scoring model after the last refinement step.

Figure S5: Results of NMR-assisted refinement of server-models in our post-CASP13 analysis

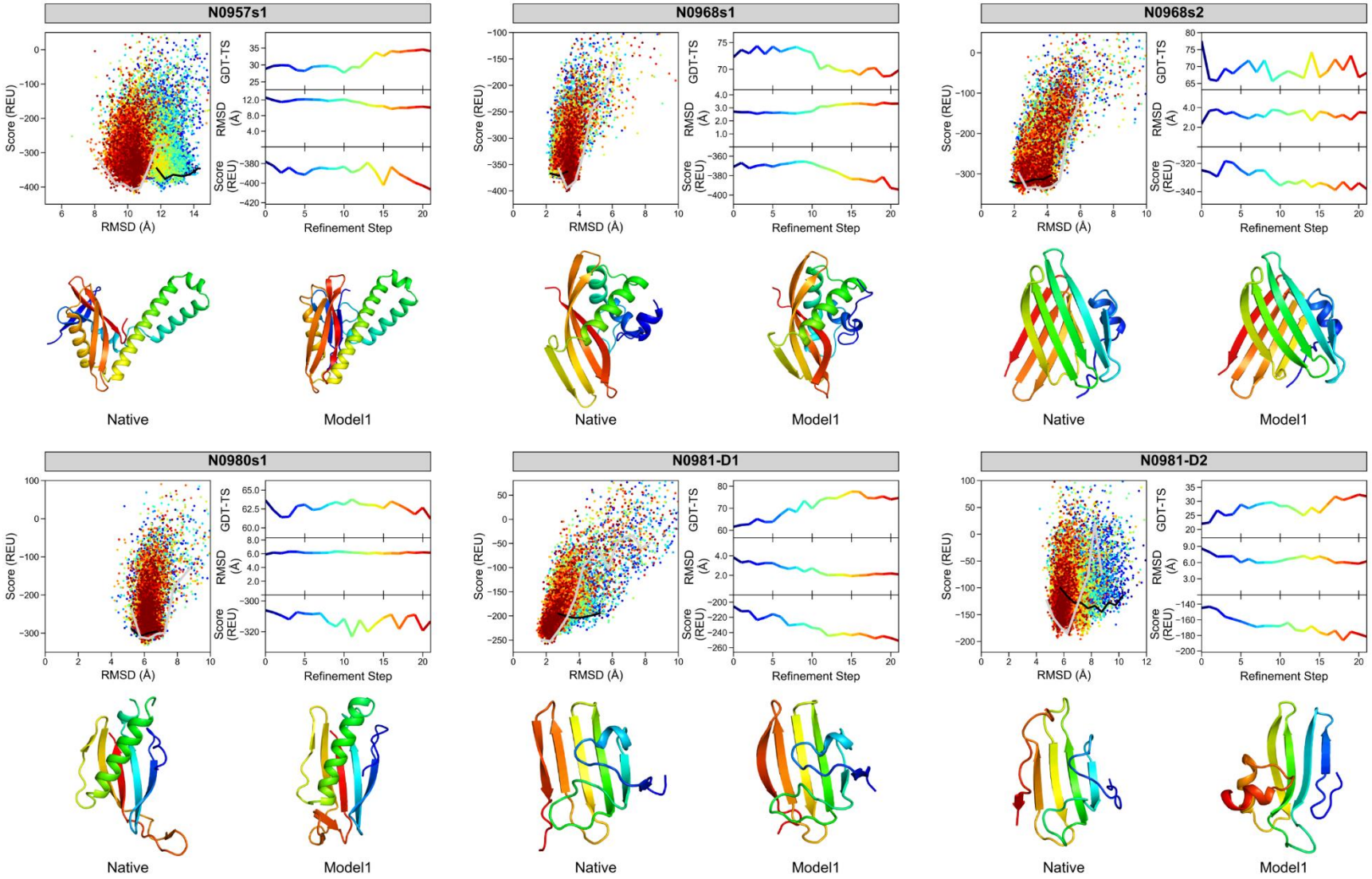

Figure S5: Results of NMR-assisted structure refinement of server-models in our post-CASP13 analysis.

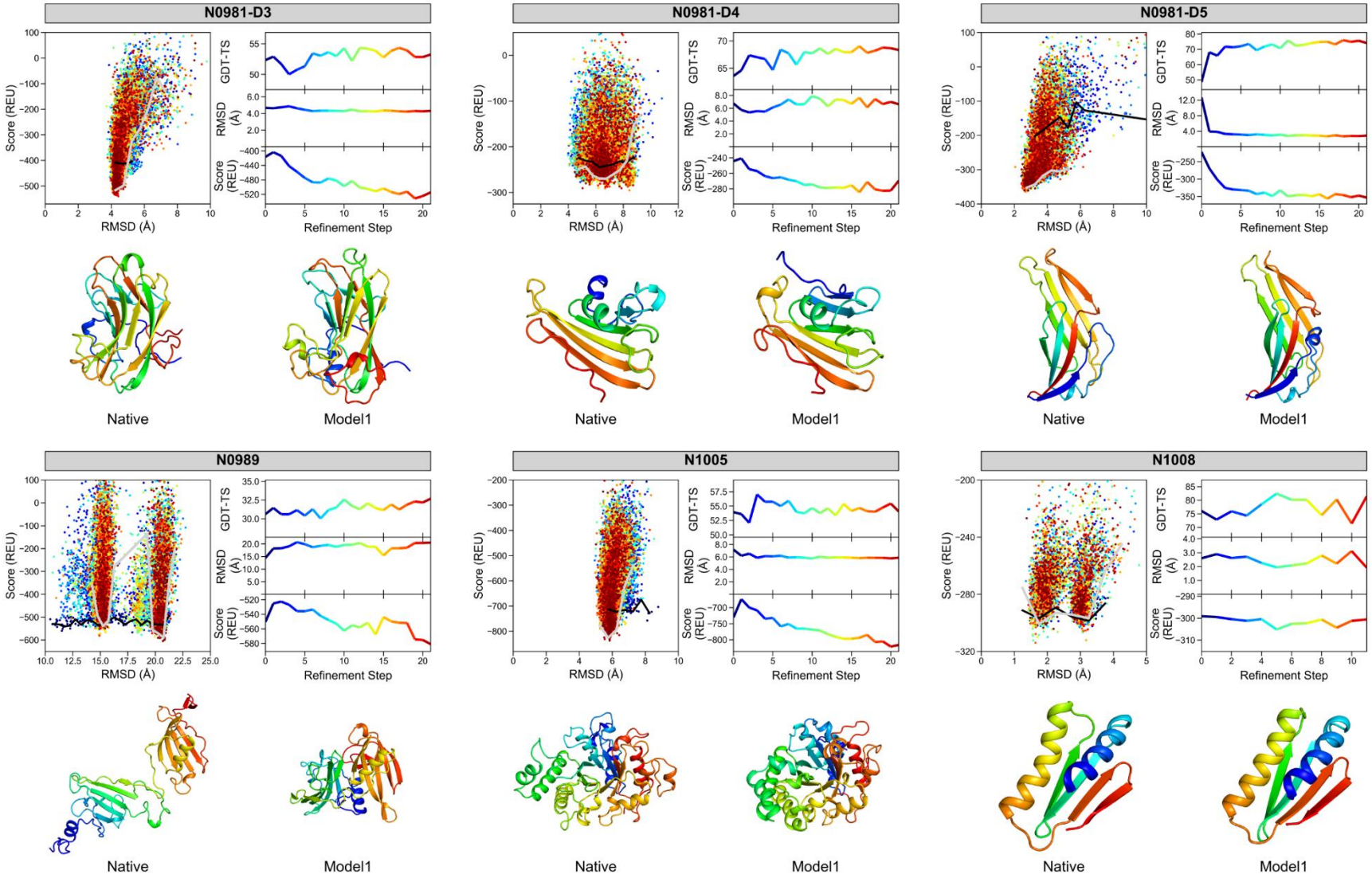

Figure S5: Results of NMR-assisted structure refinement of server-models in our post-CASP13 analysis (continued). For each of the 12 prediction targets, the top five models submitted by the I-TASSER[2,3], QUARK[4], Robetta[5], RaptorX-Contact[6] and RaptorX-TBM[7] server were combined and iteratively refined with RosettaCM and NMR (NOE+RDC) data. The arrangement of panels and the type of displayed structure evaluation metrics are the same as in **Figure S4**: The upper left panel plots the combined Rosetta energy and NMR NOE+RDC restraint score versus the model's Cα-RMSD relative to the reference structure. The upper right panel displays the average GDT-TS (top row), Cα-RMSD (middle row) and score (bottom row) of the then lowest scoring models after each refinement step. The values of successive refinement steps are colored from blue to red. The lower panel compares the experimental reference structure (left) depicted as ribbon diagram and colored in rainbow with the lowest scoring model after the last refinement step (right).

Figure S6: GDT-TS comparison of Meilerlab models to group 431 models

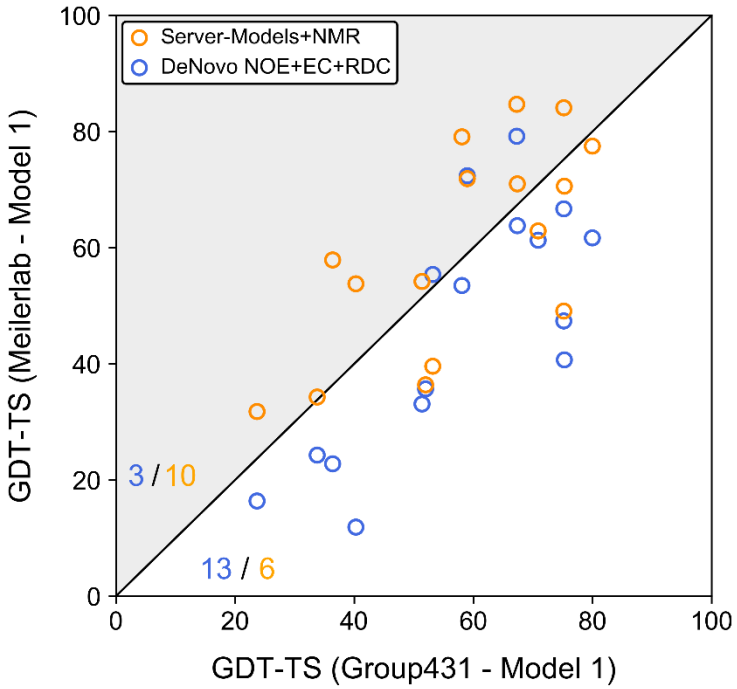

Figure S6: GDT-TS comparison of Meilerlab models to group 431 models. Comparison of GDT-TS of Meilerlab submitted Model 1 and NMR-refined server-models to Model 1 created by group 431. Gray areas indicate a higher GDT-TS of the Meilerlab model. The number of modeling cases that fell above and below the diagonal line, respectively, are indicated in the lower left corner.

Figure S7: Structure prediction of oligomeric target H0980

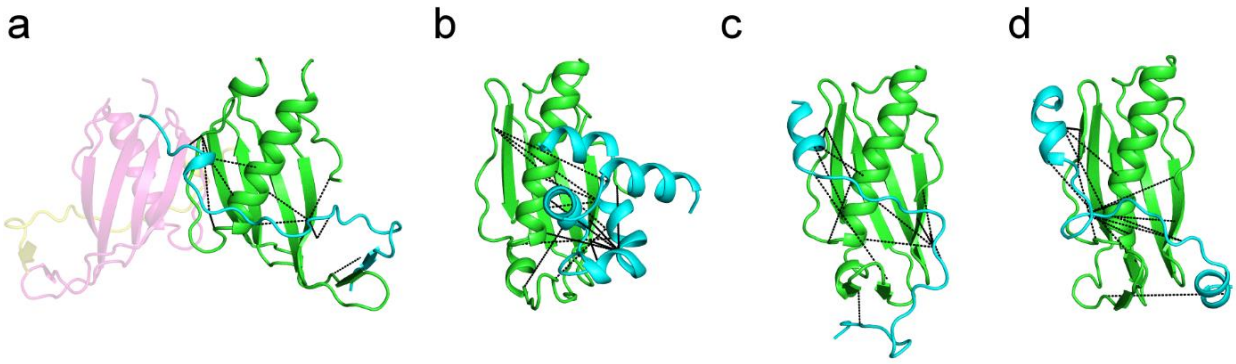

Figure S7: Structure prediction of oligomeric target H0980. (a) The asymmetric unit of the X-ray structure contains two copies of the receptor (colored green and pale magenta) and peptide (colored cyan and pale yellow) chain, displayed in cartoon representation. **(b)** Our submitted model 1 was created by (i) folding the receptor and peptide chain separately and (ii) docking both models together with RosettaDock[8] guided by intermolecular NOE distance restraints (depicted as black dotted lines) and RDCs. The peptide ligand Cα-RMSD after superimposition of the receptor was 22.7 Å. An alternative modeling strategy that we explored in our post-CASP13 analysis involved simultaneous folding and docking of the peptide onto the receptor model using Rosetta FlexPepDock[9]. The lowest-scoring FlexPepDock model **(c)** and the lowest-RMSD model **(d)** had a ligand Cα-RMSD of 16.0 Å and 12.8 Å, respectively.

Figure S8: Local model accuracy and fragment quality of *de novo* predicted NMR-assisted targets

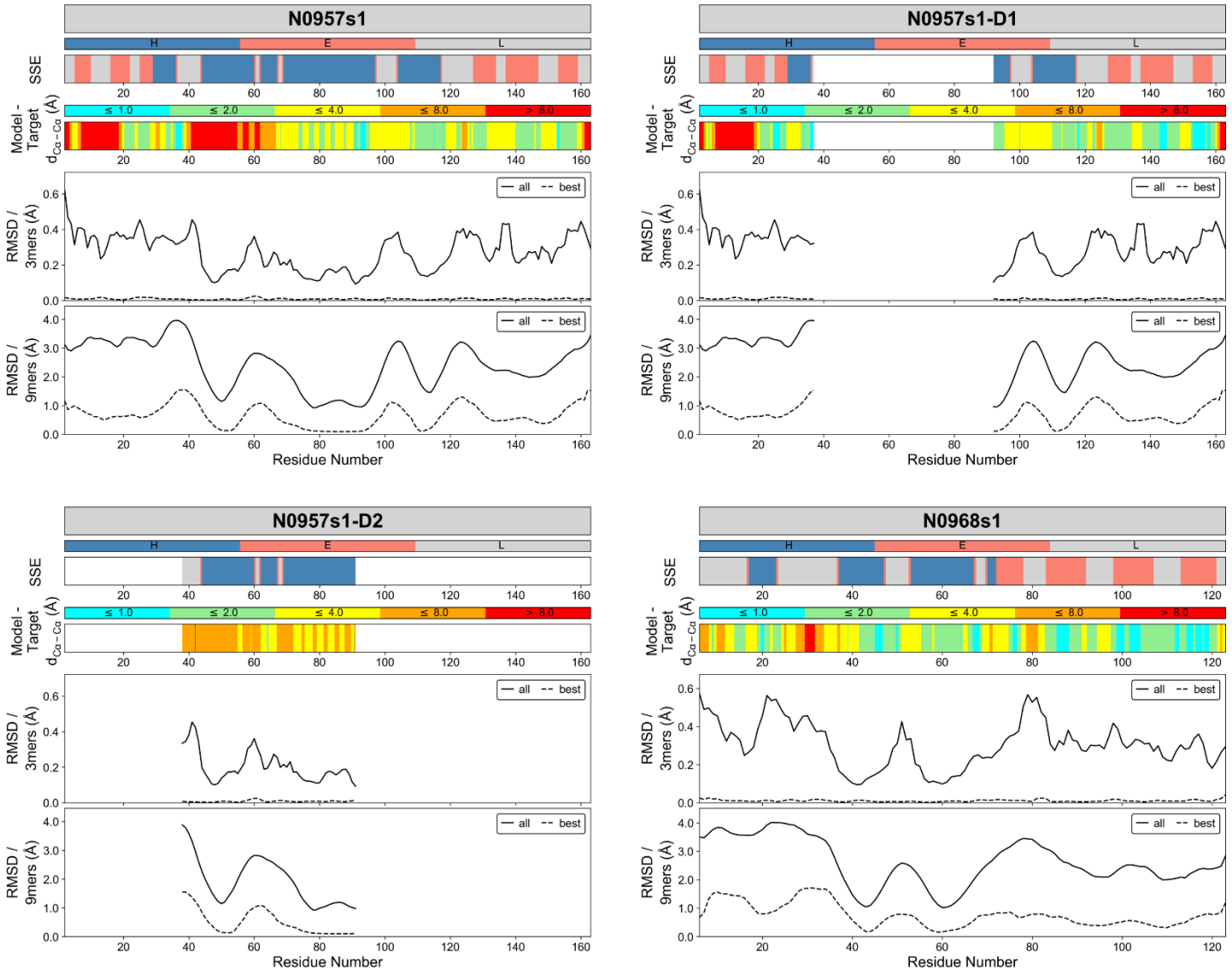

Figure S8: Comparison of local model accuracy of *de novo* predicted NMR-assisted (NOEs+RDCs) targets to Rosetta fragment quality. For each of the 12 prediction targets or 16 evaluation units, respectively, the local Cα-Cα deviation between model and reference structure is compared to the Cα-RMSD of the employed 3- and 9-residue fragments and the target secondary structure. For each target the panels display the following information: DSSP[10]-assigned secondary structure (top panel; blue: helix, salmon: sheet, gray: loop), model-target Cα-Cα distance deviation (second panel from top; cyan: ≤1Å, green: ≤2Å, yellow: ≤4Å, orange: ≤8Å, red: >8Å), Cα-RMSD of 3-residue fragments along protein sequence (second panel from bottom; solid line represents average over all 200 fragments and broken line represents lowest RMSD fragment) and Cα-RMSD of 9-residue fragments along protein sequence (bottom panel; solid line: average RMSD all fragments, broken line: lowest RMSD fragment).

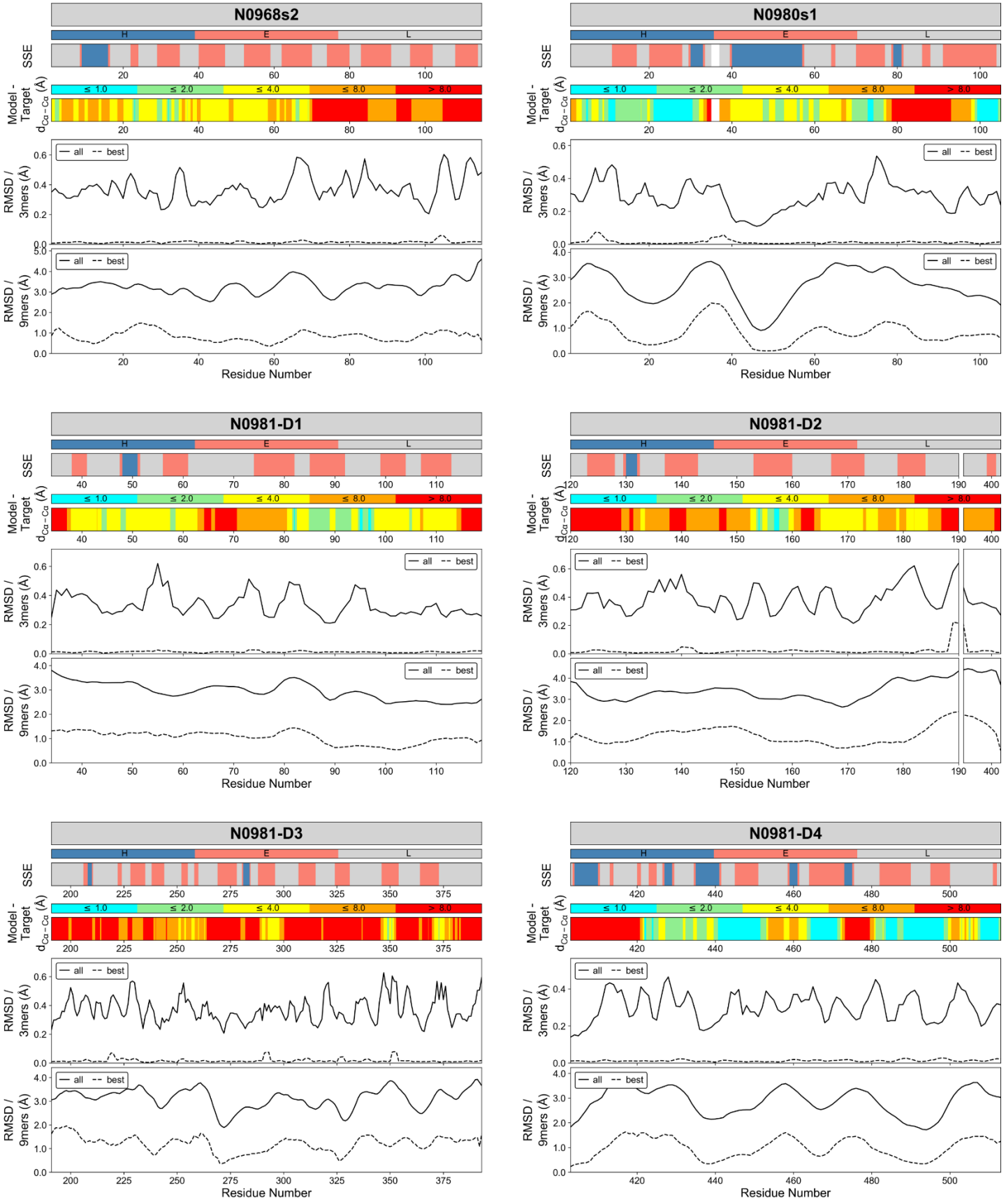

Figure S8: Comparison of local model accuracy of *de novo* predicted NMR-assisted (NOEs+RDCs) targets with Rosetta fragment quality (continued).

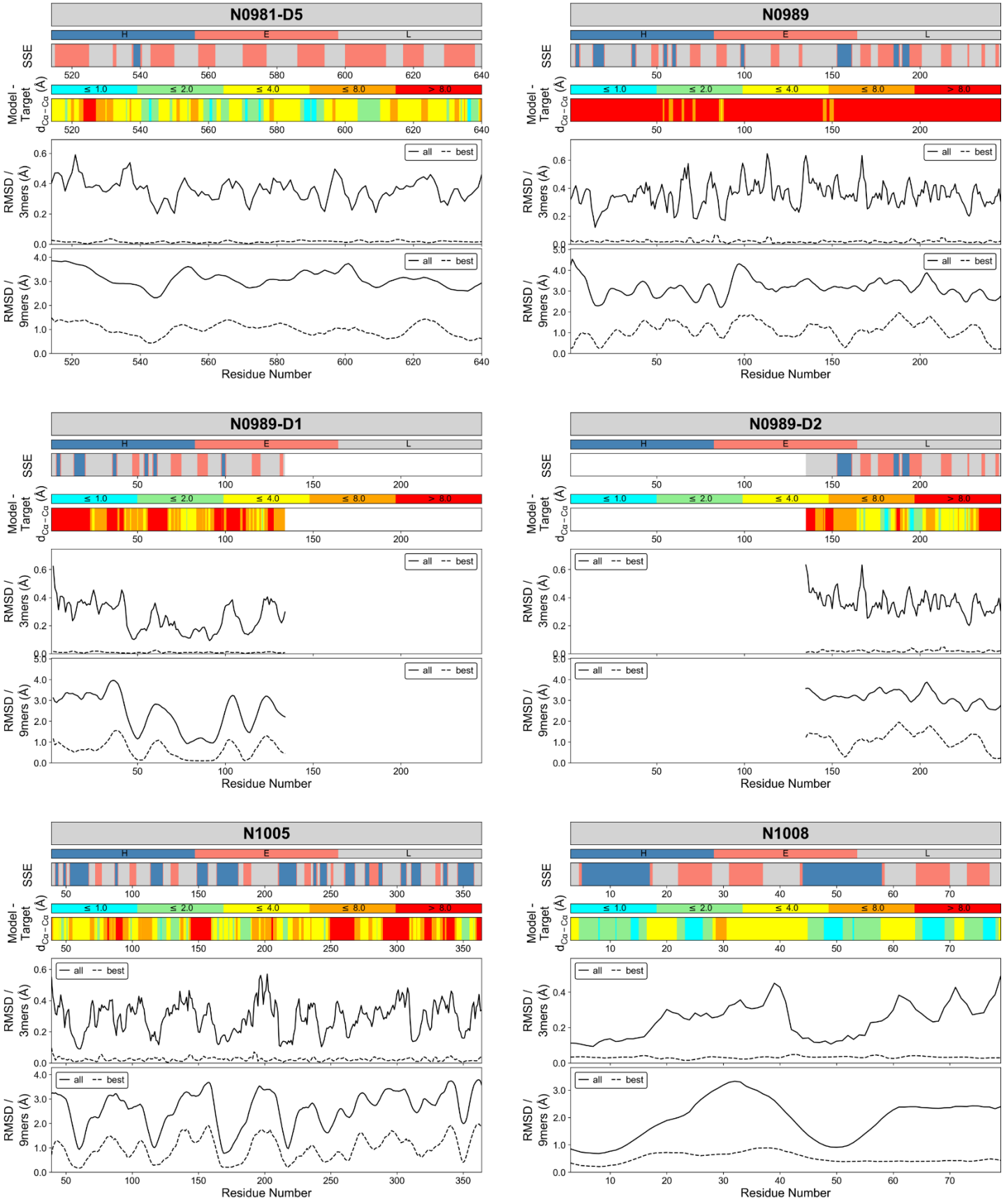

Figure S7: Comparison of local model accuracy of *de novo* predicted NMR-assisted (NOEs+RDCs) targets with Rosetta fragment quality (continued).

Supporting Tables

Table S1: Satisfied NOE contacts in submitted *de novo* models and NMR-refined server-models

Target	Residues	Reference Structure		DeNovo+NOE+RDC Submitted Model 1				NMR-refined Server-Model			
		All[#]	TP*	All[#]	TP*	Recall (%)[†]	Precision (%)[‡]	All[#]	TP*	Recall (%)[†]	Precision (%)[‡]
N1008	77	30	30	33	29	96.7	87.9	33	29	96.7	87.9
N0981-D2	80	90	90	86	65	72.2	75.6	87	66	73.3	75.9
N0981-D1	86	95	95	91	83	87.4	91.2	99	93	97.9	93.9
N0980s1	111	200	200	231	193	96.5	83.5	233	194	97.0	83.3
N0981-D4	111	171	171	184	166	97.1	90.2	185	166	97.1	89.7
N0968s2	116	161	161	180	136	84.5	75.6	168	156	96.9	92.9
N0968s1	126	143	143	142	139	97.2	97.9	144	142	99.3	98.6
N0981-D5	127	288	288	278	250	86.8	89.9	292	271	94.1	92.8
N0957s1	163	428	428	450	387	90.4	86.0	396	344	80.4	86.9
N0981-D3	203	546	546	406	255	46.7	62.8	452	361	66.1	79.9
N0989	246	327	327	290	190	58.1	65.5	381	273	83.5	71.7
N1005	326	1640	1640	1555	1285	78.4	82.6	1668	1439	87.7	86.3
Mean						**82.7**	**82.4**			**89.2**	**86.6**
Mean (-N0981-D3, -N0989)						**88.7**	**86.0**			**92.0**	**88.8**

[#]Number of all satisfied NOE contacts in restraint set. For the native reference structure all satisfied NOE contacts are considered TP-NOEs.
*Number of satisfied TP-NOE contacts in restraint set.
[†]Recall is ratio of TP-NOE contacts in Rosetta model vs. TP-NOE contacts in reference structure.
[‡]Precision is ratio of satisfied TP-NOE contacts vs. all satisfied NOE contacts in Rosetta model.

Table S2: RDC Q-factor (%) of submitted *de novo* models and NMR-refined server-models

Target	Residues	DeNovo+RDC submitted Model 1	DeNovo+NOE+RDC submitted Model 1	NMR-refined Server-Model
N1008*	77	-	-	-
N0981-D2	80	31.2	38.8	44.6
N0981-D1	86	37.0	30.1	28.9
N0980s1	111	45.3	36.7	32.8
N0981-D4	111	57.5	51.3	62.2
N0968s2	116	38.9	33.2	25.4
N0968s1	126	40.7	37.5	36.3
N0981-D5	127	55.0	51.2	30.7
N0957s1	163	44.4	42.4	53.4
N0981-D3	203	67.9	84.8	60.8
N0989	246	52.7	49.4	38.3
N1005	326	72.8	66.6	56.8
Mean		**49.4**	**47.4**	**42.7**
Mean (-N0981-D3, -N0989)		**47.0**	**43.1**	**41.2**

*No RDC data were available for target N1008

Supporting References

1. Ortiz AR, Strauss CEM, Olmea O. MAMMOTH (Matching molecular models obtained from theory): An automated method for model comparison. *Protein Sci.* 2002;11:2606-2611.
2. Zhang Y. I-TASSER server for protein 3D structure prediction. *BMC Bioinformatics.* 2008;9:40.
3. Yang J, Yan R, Roy A, Xu D, Poisson J, Zhang Y. The I-TASSER Suite: protein structure and function prediction. *Nat Methods.* 2015;12(1):7-8.
4. Xu D, Zhang Y. Ab initio protein structure assembly using continuous structure fragments and optimized knowledge-based force field. *Proteins.* 2012;80(7):1715-1735.
5. Kim DE, Chivian D, Baker D. Protein structure prediction and analysis using the Robetta server. *Nucleic Acids Res.* 2004;32(Web Server issue):W526-531.
6. Wang S, Sun S, Xu J. Analysis of deep learning methods for blind protein contact prediction in CASP12. *Proteins.* 2018;86 Suppl 1:67-77.
7. Källberg M, Wang H, Wang S, et al. Template-based protein structure modeling using the RaptorX web server. *Nat Protoc.* 2012;7(8):1511-1522.
8. Gray JJ, Moughon S, Wang C, et al. Protein-protein docking with simultaneous optimization of rigid-body displacement and side-chain conformations. *J Mol Biol.* 2003;331(1):281-299.
9. Raveh B, London N, Schueler-Furman O. Sub-angstrom modeling of complexes between flexible peptides and globular proteins. *Proteins.* 2010;78(9):2029-2040.
10. Kabsch W, Sander C. Dictionary of Protein Secondary Structure: Pattern Recognition of Hydrogen-Bonded and Geometrical Features. *Biopolymers.* 1983;22:2577-2637.